ELSEVIER

Tectonophysics 308 (1999) 205–221

TECTONOPHYSICS

www.elsevier.com/locate/tecto

Rupture zones in the Aegean region

B.C. Papazachos [a,*], C.A. Papaioannou [b], C.B. Papazachos [b], A.S. Savvaidis [a]

[a] *Geophysical Laboratory, University of Thessaloniki, P.O. Box 352-1, GR-54006 Thessaloniki, Greece*
[b] *Institute of Engineering Seismology and Earthquake Engineering (ITSAK), P.O. Box 53, Foinikas, GR-55102 Thessaloniki, Greece*

Received 19 December 1997; accepted 25 August 1998

Abstract

Rupture zones of strong shallow earthquakes can be investigated by field observations of surface fault traces (SF), accurate location of spatial clusters of aftershocks or other small earthquakes (CL), reliable fault plane solutions (FP) and information on the spatial distribution of sites with high ($I \geq$ VIII) macroseismic intensities (MA). The validity of these four techniques was successfully tested by comparing the results of their application to several cases of strong shallow earthquakes. These techniques were then applied to spatially define the rupture zones of 150 strong ($M \geq 6.0$) shallow earthquakes in the Aegean and surrounding area. The type of faulting was determined for all these zones by the use of reliable fault plane solutions, which are available for this area. The orientation of most of these rupture (fault) zones is in good agreement with the presently acting stress field with some exceptions which are attributed to the rupture of pre-existing faults. The tectonic implications of these zones are discussed.

Keywords: rupture zones; Aegean area; macroseismic data; stress-field

1. Introduction

The rupture zone of an earthquake is usually considered to be the part of the Earth's lithosphere, which is strongly deformed before the earthquake (Benioff, 1955, 1962; Gzovsky, 1962), that ruptures during the generation of the earthquake. It is also assumed that the foci of aftershocks of a shallow mainshock are due to redistribution of the stress in the rupture zone, caused by the generation of the mainshock, and for this reason the spatial distribution of aftershocks defines the rupture zone of the mainshock (Benioff, 1955; Kiratzi et al., 1985). In addition to the location of aftershocks, other methods have been used to estimate the extent of rupture zones of past strong shallow earthquakes such as locations of crustal uplift or subsidence, surface faulting, damage distribution, heights of seismic sea waves along nearby coastlines and places with high values of macroseismic intensities (Kelleher, 1972).

In the present study, we focus our attention on the rupture zones of strong earthquakes in the Aegean area. Fig. 1 shows the main topographic features of tectonic origin in this area (Papazachos and Papazachou, 1997). Typical features of a subduction zone are observed in the southern Aegean along the Hellenic arc, with an outer-arc trench (Hellenic trench), a thick-crust accretionary prism (Hellenides mountain chain–main axis of Alpine folding), a back-arc trough (South Aegean trough) and an inner-arc vol-

* Corresponding author. E-mail: elpapadimi@olymp.ccf.auth.gr

0040-1951/99/$ – see front matter
PII: S0040-1951(99)00073-6

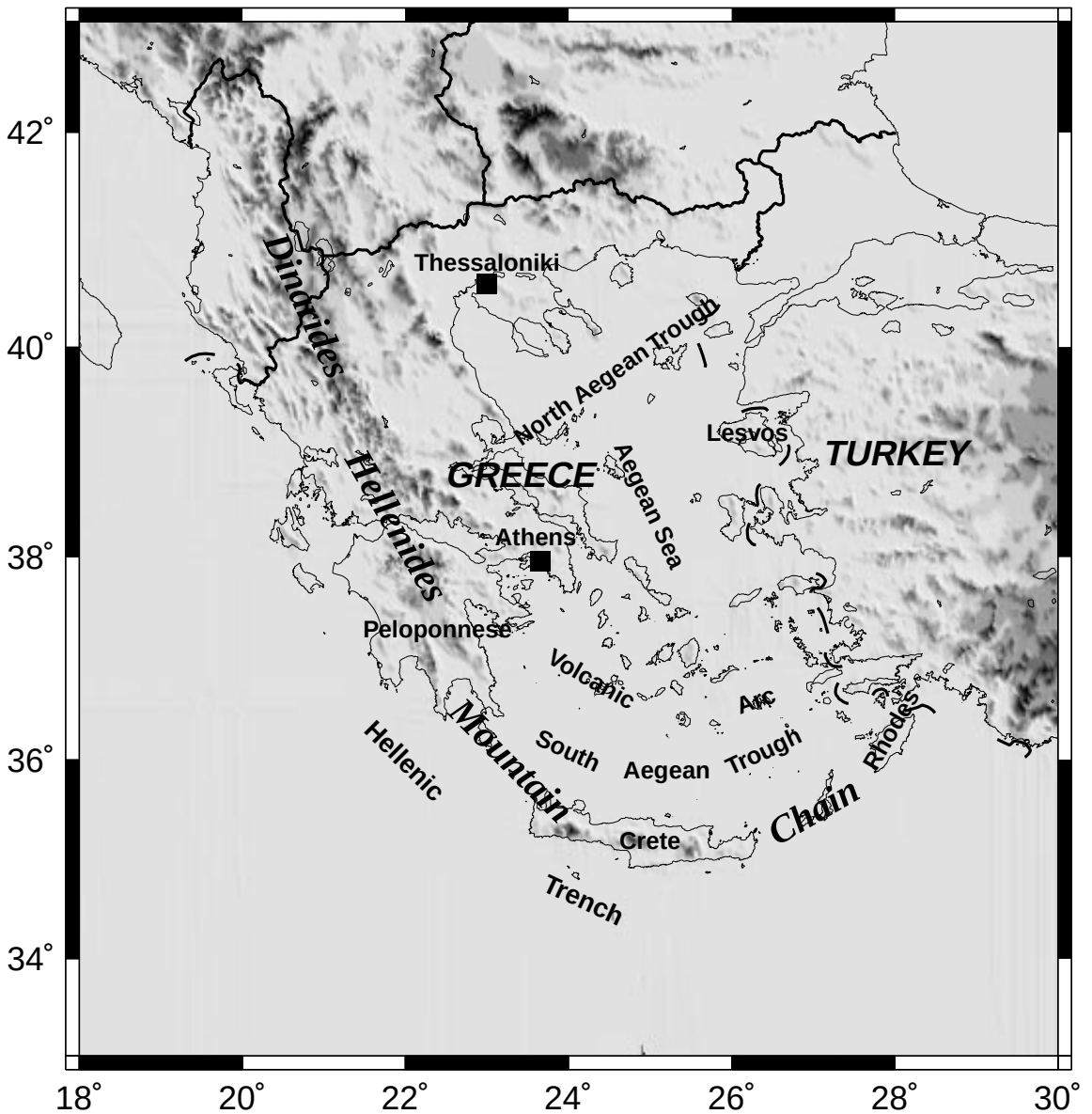

Fig. 1. Topographic features of tectonic origin in the Aegean and surrounding area.

canic arc. The North Aegean is characterised by the presence of a large NE–SW trending trough, the North Aegean trough, which represents the continuation of the dextral North Anatolia fault into the Aegean.

Rupture zones of several strong earthquakes in Greece have been defined by the use of field observations of fault traces (FT) and by precise location of clusters (CL) of aftershocks or other relatively small earthquakes. Such data have already been used (Papazachos, 1989) to derive the following relations between the fault length, L (in km), and the fault width, w (in km), as a function of the 'equivalent' moment magnitude M (original M_w or determined from other magnitude estimates; Papazachos et al., 1997a):

$$\log L = 0.51M - 1.85 \quad (1)$$

$$\log w = 0.19M - 0.13 \quad (2)$$

Fault plane solutions (FP) have been also used to define the strike and dip of the rupture zones of strong shallow earthquakes of this area. Moreover, it is possible to determine the length and the width of the zone using Eqs. 1 and 2. However, rupture zones can be defined using the spatial clustering of earthquakes (aftershocks, etc.) or fault plane solutions only for the strong earthquakes which occurred during the last four decades, because such reliable data are available only for these earthquakes. On the other hand, accurate field observations on surface fault traces in the Aegean are available only for a small number of strong earthquakes of the last two centuries (Papazachos and Papazachou, 1997). It is, therefore, necessary to seek for alternative methods to define rupture zones of older strong earthquakes for which no reliable data are available on surface fault traces, clustering of smaller shocks (aftershocks, etc.) and focal mechanisms. One such method relies on the use of macroseismic data since evidence has been presented (Kelleher, 1972) that the meizoseismal area of a strong shallow earthquake defines the horizontal extent of its rupture zone.

Accurate location and definition of the properties of rupture zones are of importance for both practical purposes (seismic hazard assessment, etc.) as well as for theoretical modelling (seismotectonic models, etc.). For this reason, the reliability of the methods previously mentioned for defining rupture zones is tested by applying them to 45 earthquakes and comparing their results. These methods are then applied to define the rupture zones of 150 strong ($M \geq 6.0$) shallow ($h < 60$ km) earthquakes in the Aegean and surrounding area (34ºN–43ºN, 19ºE–30ºE). The seismotectonic implications of these results are discussed.

2. Comparison of rupture zones in Greece defined with different techniques: recent examples

In order to define rupture zones in the area of Greece, all kind of relative information (fault planes solutions, fault traces, clustering of foreshocks and aftershocks) have been used. Moreover, recently published macroseismic data for the broader Aegean area (Papazachos et al., 1997b) were also used. Papazachos (1992) has developed a method for estimating synthetic isoseismals (of approximately elliptical shape) which is based on the use of near field macroseismic observations (high macroseismic intensities). In this method the anisotropic radiation at the source, geometrical spreading and anelastic attenuation are taken into account. Application of this method for three earthquakes in Southern Thessalia (1954, $M = 7.0$, 1957 $M = 6.8$, 1980 $M = 6.5$), for which information for their rupture zones was available from other sources (ground deformations, geological observations, spatial distributions of aftershocks), showed that the estimated isoseismal of intensity VIII (in the MM scale) correlated very well with the horizontal extent of the boundary of the rupture zones (Caputo and Pavlides, 1991; Papazachos et al., 1993) and that the direction of the major axis of the isoseismals was parallel to the strikes of the faults. This agreement suggests that the direction of maximum energy radiation which is estimated from the isoseismals correlates very well with the direction of the rupture, hence macroseismic information can be used to determine this direction.

In order to test the compatibility of the previously mentioned techniques, we studied several cases where more than one kind of the previously described information was available. The rupture zones of three strong shallow earthquakes which occurred recently in Greece (Thessaloniki 1978, $M = 6.5$; Alkyonides 1981, $M = 6.7$; Kalamata 1986, $M = 6.0$) have been reliably defined by observations of clear surface fault traces (FT), accurate location of aftershocks (CL), reliable fault plane solutions (FP), as well as by geological and geomorphological information in each case (Soufleris and Stewart, 1981; Mountrakis et al., 1983; Papazachos et al., 1984a, 1988; Lyon-Caen et al., 1988). Reliable determination of the rupture zones of five other strong recent shallow earthquakes (Montenegro 1979, $M = 7.1$; Magnesia 1980, $M = 6.5$; N Aegean 1981, $M = 7.2$; Cephalonia 1983, $M = 7.0$; Kozani 1995, $M = 6.6$) of this area, for which geological and geomorphological information was available has been also made by two of the previ-

ously mentioned seismological methods (CL, FP), that is by accurate location of aftershocks and by reliable fault plane solutions, since no information for surface trace of the mainshock fault exists for these cases (Papazachos et al., 1983, 1984b; Karakaisis et al., 1985; Scordilis et al., 1985; Hatzfeld et al., 1996).

In all the previous cases, the agreement between the results of the different methods employed for the determination of the rupture zone (FP, FT, CL) was excellent. Moreover, the directivity of macroseismic data (MA) determined by the previous procedure was also in very good agreement with the results of the other methods. A typical example is the Kalamata 1986, $M = 6.0$ earthquake which is among the recent strong earthquakes for which all types of information was available. The comparison of the different techniques is shown in Fig. 2. A clear NNE–SSW direction of the rupture zone is identified in all data sets (neotectonic fault and surface ruptures, fault plane solution, aftershock sequence, direction of the isoseismals).

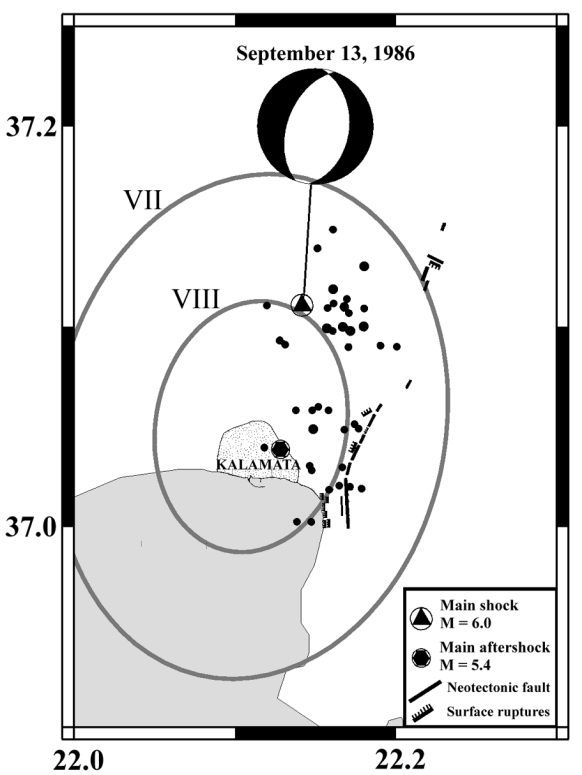

Fig. 2. Comparison of the direction of the fault rupture determined from different information for the September 19, 1986, $M = 6.0$ Kalamata event (southern Greece). The fault plane solution, distribution of aftershock foci (black circles), as well as the neotectonic fault and various surface ruptures created by the main event (Papazachos et al., 1988) are shown in this figure. The synthetic isoseismals of macroseismic intensity VIII and VII, in MM scale, (Papazachos et al., 1997b) are also superimposed. All types of data show the same NNE–SSW (~200°) rupture zone direction.

Another interesting example is the rupture zone of the Kozani 1995 ($M = 6.6$) earthquake which has been defined and investigated in detail by the use of seismological, geological and geodetic data (Pavlides et al., 1995; Hatzfeld et al., 1996; Clark et al., 1997). The fit between near-source macroseismic observations and the estimated synthetic isoseismals (Papazachos, 1992) is shown on the left part of Fig. 3. The right part of the same figure shows the comparison of the different information about the rupture zone. In this case the estimated isoseismal of intensity VIII also correlated well with the horizontal extent of the rupture zone (Papazachos et al., 1998). It should be noted that the surface ruptures seen in Fig. 3 were not clearly identified as the surface expression of the fault (Pavlides et al., 1995), but the correlation observed in Fig. 3 further supports this scenario.

3. Validation of the techniques

The four techniques applied in this paper can be separated into two categories, depending on the kind of the input seismological observations. Two of these techniques (SF, MA) are based on near field observations (surface fault traces, macroseismic effects of earthquakes near the epicenter) and can give information on the horizontal dimensions of the rupture zone. The other two techniques (CL, FP) are based on far field observations (travel times of waves for locating aftershocks, first onsets and waveform modelling to determine fault plane solutions) and give additional information for the three-dimensional geometry of the rupture zone. None of these techniques alone provides all the necessary information for the rupture zone, that is the full geometry (strike, dip), type (thrust, normal, strike-slip) and dimensions (length, width) of the rupture zone of

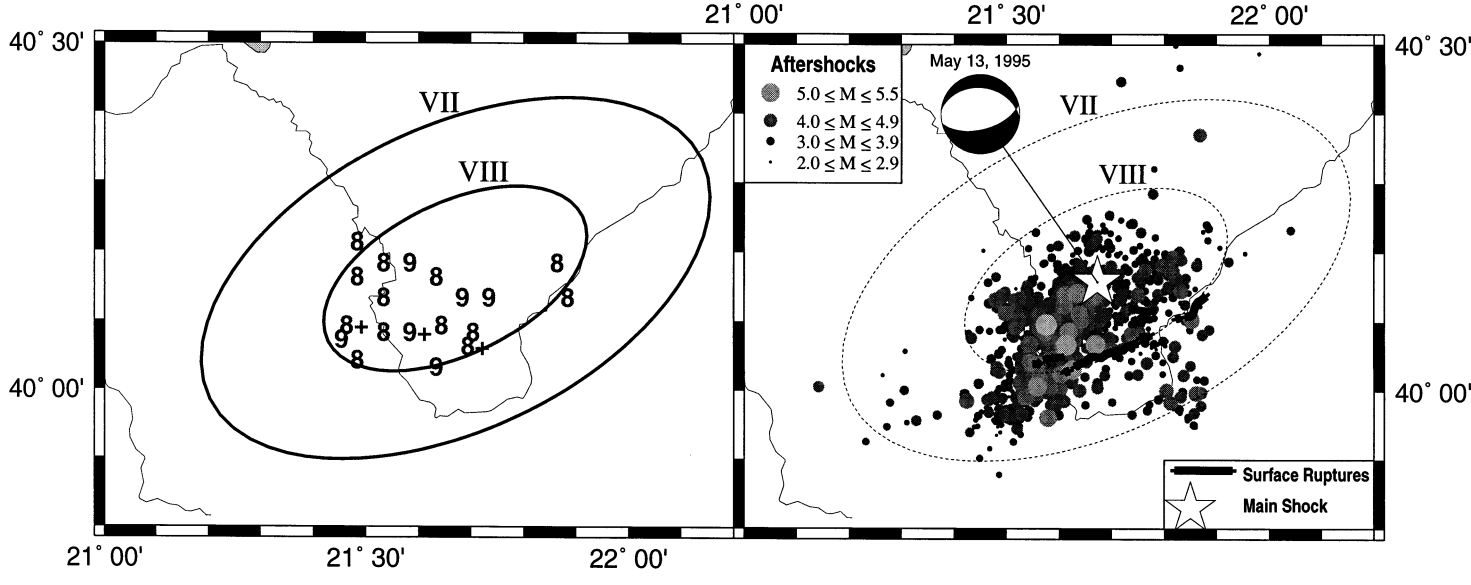

Fig. 3. Rupture zone of the May 13, 1995, $M = 6.6$ Kozani event (northern Greece) determined from different data. On the left figure, the synthetic isoseismals of macroseismic intensity VIII and VII, in MM scale (Papazachos et al., 1997b) and the fit of the isoseismal of intensity VIII with the original macroseismic observations is shown. On the right figure the relocated epicentres of the aftershock sequence (Papazachos et al., 1998), fault plane solution (Geological Survey of Japan), surface ruptures (Pavlides et al., 1995) are presented with the synthetic isoseismals superimposed (dashed lines). The agreement of the rupture zone directivity (~240°) between the different data sets is very good.

an earthquake, unless it is combined with the others or some other kind of information (geological, geomorphological, lithospheric kinematics, etc.).

However, each one of these techniques can be used to define the strike of the rupture zone since it is assumed, as mentioned above, that surface fault traces are parallel to the strike of the fault plane, aftershocks and other small earthquakes are due to redistribution of the stress in the rupture zone, one of the nodal planes of a fault plane solution is the fault plane, and that the major axis of the meizoseismal area of a shallow earthquake (area where the macroseismic intensity is $I \geq$ VIII in the MM scale) is parallel to the strike of the fault. Additional information which support these assumptions are presented here.

A simple way to test the validity of these assumptions is to apply these techniques (SF, MA, CL, FP) to the same earthquake and compare the results for several earthquakes. This application also allows the estimation of the uncertainty in the calculation of the strike of the rupture zone. Table 1 presents the basic information (date, geographic coordinates of the epicenter, moment magnitude) for 45 shallow strong ($M \geq 6.0$) earthquakes. For each earthquake at least two of these techniques (SF, MA, CL, FP) have been applied to calculate the strike of its rupture zone. The values of the calculated strikes (in degrees) and the corresponding references from which these values have been taken are also listed in the table.

The surface fault strikes are listed in column SF of Table 1 for 14 earthquakes for which reliable field observations have been made. For each of these cases the length of the observed fault trace is found comparable with the fault length given by Eq. 1. Also, the azimuth of the maximum axis of the isoseismals with $I >$ VIII is given in column MA for 44 shocks listed in Table 1. These isoseismals together with the corresponding observed macroseismic intensities are listed in the new isoseismal map of shallow earthquakes of the Aegean area (Papazachos et al., 1997b). The synthetic isoseismals have been estimated by an appropriate method which takes into account the anisotropic radiation at the focus, geometrical spreading and anelastic attenuation (Papazachos, 1992).

For 12 earthquakes listed in Table 1, clusters of small shocks (aftershocks, etc.) related to them were available. The epicentres of these small shocks are clustered along a more or less linear segment. The azimuth of this line is given in column CL (cluster) of this table. Finally, for 38 earthquakes of Table 1 reliable fault plane solutions were available. The distinction between the fault plane and the auxiliary plane was made on the basis of several independent observations (geological, lithospheric kinematics, etc.). The strikes of the fault planes are listed in column FP of Table 1.

Based on the data of Table 1 the values of all possible differences in the strikes (SF–MA, SF–CL, SF–FP, MA–CL, MA–FP, CL–FP) were calculated for each earthquake. The mean value of these differences (85 values) is close to zero (-1^o) with a standard deviation of 15^o. Examination of the frequency distribution of each one of the six differences mentioned above does not give any clear evidence for superiority or inferiority of anyone of the four techniques. However, comparison of the results obtained by the two near field observational techniques (SF, MA) and those obtained by the two far field instrumental techniques (CL, FP) shows that the strikes determined are more compatible for each group. Hence, the frequency distribution of such differences (14 values of SF–MA and 12 values of CL–FP) has a mean value close to zero (-2^o) and a standard deviation of $\sigma_1 = 13^o$. When the results of near field techniques are compared with the results of the far field techniques the standard deviation is larger ($\sigma = 17^o$), although the mean value is still close to zero (1^o). It is also interesting to notice, that the residuals of the macroseismic method from all other techniques result in an average value of -2^o and a standard deviation of 16^o which is comparable with the global standard deviation. This agreement suggests that this method can be practically applied for the determination of the rupture zone direction, especially for historical events, without reducing significantly the accuracy of the estimation compared to the other techniques.

4. The stress field in the Aegean area

On the basis of typical fault plane solutions determined by Papazachos et al. (1997c) for several clusters of strong shallow earthquakes and by the use of additional data concerning surface fault traces,

Table 1
Date, epicenter, moment magnitude and estimated strikes (SF, MA, CL, FP in degrees), by at least two of the four techniques, for 45 shallow earthquakes

No.	Date	φ°_{N}, λ°_{E}	M	SF	MA	CL	FP	Ref.
1	1861, Dec. 26	38.25, 22.16	6.7	285	288	–	–	1,2
2	1894, Apr. 20	38.60, 23.04	6.7	295	309	–	–	3,2
3	1894, Apr. 27	38.66, 23.04	7.2	295	323	–	–	3,2
4	1928, Apr. 14	42.15, 25.28	6.8	90	87	–	–	3,2
5	1928, Apr. 18	42.10, 25.00	7.0	270	270	–	–	3,2
6	1932, Sep. 26	40.45, 23.76	7.0	90	110	–	–	4,2
7	1953, Mar. 18	40.02, 27.53	7.4	250	259	–	–	3,2
8	1956, July 9	36.64, 25.96	7.5	–	74	60	65	2,5,6
9	1963, Sep. 18	40.67, 29.00	6.3	–	277	–	293	2,7
10	1964, Oct. 6	40.10, 27.93	6.9	280	271	–	273	9,2,8
11	1965, Mar. 9	39.16, 23.89	6.1	–	52	–	40	2,10
12	1965, Apr. 5	37.70, 22.00	6.1	–	220	–	226	2,10
13	1965, July 6	38.27, 22.30	6.3	–	253	–	281	2,11
14	1966, Feb. 5	39.10, 21.70	6.2	–	90	–	90	2,11
15	1966, Oct. 29	38.78, 21.11	6.0	–	324	–	324	2,11
16	1967, Mar. 4	39.20, 24.60	6.6	–	90	–	98	2,10
17	1967, May 1	39.47, 21.25	6.4	–	351	–	2	2,8
18	1967, Nov. 30	41.39, 20.46	6.3	–	19	–	4	2,11
19	1968, Feb. 19	39.50, 25.00	7.1	–	211	–	217	2,12
20	1969, Jan. 14	36.10, 29.20	6.2	–	290	–	282	2,10
21	1969, Mar. 3	40.10, 27.50	6.0	–	286	–	268	2,7
22	1969, Mar. 23	39.13, 28.44	6.1	–	137	–	112	2,13
23	1969, Mar. 28	38.29, 28.57	6.6	290	292	–	281	31,2,13
24	1970, Mar. 28	39.16, 29.42	7.1	280	287	–	308	31,2,14
25	1970, Apr. 8	38.36, 22.53	6.2	–	291	–	278	2,14
26	1970, Apr.19	39.00, 29.80	6.0	–	98	–	104	2,13
27	1972, May 4	35.10, 23.60	6.5	–	308	–	308	2,15
28	1972, Sep. 17	38.11, 20.31	6.3	–	45	–	46	2,16
29	1973, Nov. 29	35.18, 23.75	6.0	–	298	–	316	2,14
30	1978, Jun. 20	40.61, 23.27	6.5	250	242	280	278	17,2,18,19
31	1979, Apr. 15	41.97, 19.00	7.1	–	–	320	317	20,11
32	1980, July 9	39.27, 22.83	6.5	–	56	90	81	2,21,21
33	1981, Feb. 24	38.07, 23.00	6.7	260	275	260	264	22,2,22,7
34	1981, Mar. 4	38.18, 23.24	6.3	70	101	80	50	22,2,22,7
35	1981, Dec. 19	39.00, 25.26	7.2	–	40	40	37	2,23,23
36	1982, Jan. 18	39.78, 24.50	7.0	–	237	235	233	2,23,7
37	1983, Jan. 17	38.10, 20.20	7.0	–	35	30	40	2,24,24
38	1983, July 5	40.30, 27.20	6.1	–	261	–	248	2,25
39	1983, Aug. 6	40.00, 24.70	6.8	–	229	240	228	2,27,26
40	1986, Sep. 13	37.05, 22.11	6.0	200	195	200	200	28,2,28,28
41	1988, Oct. 16	37.90, 20.90	6.0	–	30	–	32	2,26
42	1990, Dec. 21	40.92, 22.36	6.0	–	75	–	45	2,26
43	1992, Nov. 6	38.19, 27.05	6.2	–	244	–	238	2,26
44	1995, May 13	40.16, 21.67	6.6	–	244	240	240	2,29,30
45	1995, June 15	38.37, 22.15	6.4	–	270	–	276	2,26

1. Schmidt (1867), 2. Papazachos et al. (1997b), 3. Richter (1958), 4. Maravelakis (1933), 5. Papazachos and Panagiotopoulos (1993), 6. Shirokova (1972), 7. Taymaz et al. (1991), 8. Papazachos et al. (1991), 9. Ambraseys (1988), 10. McKenzie (1972), 11. Baker et al. (1997), 12. Kiratzi et al. (1991), 13. Eyidogan and Jackson (1985), 14. McKenzie (1978), 15. Kiratzi and Langston (1989), 16. Papadimitriou (1993), 17. Kiratzi et al. (1985), 18, Mountrakis et al. (1983), 19. Soufleris and Stewart (1981), 20. Karakaisis et al. (1985), 21. Papazachos et al. (1983), 22. Papazachos et al. (1984a), 23. Papazachos et al. (1984b), 24. Scordilis et al. (1985), 25. Dziewonski et al. (1984), 26. Harvard Solution, 27. Rocca et al. (1985), 28. Papazachos et al. (1988), 29. Papazachos et al. (1998), 30. Geological Survey of Japan, 31. Kudo (1983).

Table 2
The azimuth, ζ, and the plunge, ϑ, of the P and T axes at the centers (φ, λ) of 36 earthquakes clusters

CL	φ°_{N}	λ°_{E}	P		T	
			ζ	ϑ	ζ	ϑ
A1	42.2	18.9	230	27	47	63
A2	41.1	19.7	241	18	96	68
A3	40.2	19.8	242	10	72	66
A4	39.3	20.6	242	2	352	84
H1	37.6	20.5	229	25	23	62
H2	37.1	21.2	215	19	353	65
H3	35.8	22.0	204	9	354	80
H4	35.0	23.7	208	27	22	62
H5	34.4	25.7	200	11	354	78
H6	35.3	27.8	200	18	5	71
H7	36.1	29.2	188	20	2	70
M1	41.4	20.4	353	83	98	2
M2	39.9	20.8	6	81	100	2
M3	39.5	21.2	189	79	285	1
M4	37.1	22.2	82	71	284	5
M5	35.6	23.5	92	71	285	18
M6	35.1	26.5	247	80	105	8
M7	36.3	27.0	226	78	117	4
T1	42.0	25.0	58	85	10	8
T2	42.0	23.0	285	82	160	8
T3	40.8	23.5	338	82	162	8
T4	40.5	21.9	231	83	337	2
T5	39.2	22.9	143	89	352	1
T6	38.3	22.2	99	78	170	2
T7	37.1	24.8	60	86	165	2
T8	36.6	26.3	75	88	166	0
T9	37.0	28.1	221	82	6	7
T10	37.7	29.4	167	81	352	9
T11	39.0	28.5	275	85	8	0
T12	39.1	29.7	228	87	15	3
S1	40.6	27.6	114	42	22	2
S2	40.0	26.2	106	28	16	3
S3	39.4	24.6	98	13	10	5
S4	38.6	26.6	92	63	193	5
S5	37.95	21.1	75	41	173	10
S6	38.3	20.3	259	12	358	35

spatial clustering of relatively small earthquakes (aftershocks, etc.) and macroseismic information, we can extend the estimation of the stress field to areas where the stress field is not known on the basis of the similarity of rupture zone directions. Using this correlation, the typical orientations of the P (maximum compression) and T (maximum tension) axes have been reliably determined at 36 sites of the Aegean and surrounding area. Table 2 shows the geographic coordinates of these 36 sites and the corresponding typical azimuths, ζ, and plunges, ϑ, of the P and T axes. The horizontal projections of the P (black arrows) and of the T (white arrows) vectors are shown in Fig. 4. In the cases where one of the major stress axes was sub-vertical, its horizontal projection is not plotted. Several stress field regimes are observed in this figure and are discussed below.

5. Seismic faults and rupture zones

All the available information which concerns fault plane solutions, surface fault traces, spatial clustering of relatively small earthquakes and macroseismic observations, were used to define fault parameters of 150 shallow strong ($M \geq 6.0$) earthquakes in the Aegean and surrounding area which are shown in Table 3. In the first four columns of this table the code number, date, geographic coordinates of the epicentre and the magnitude of the corresponding earthquake are given. In the next three columns the strike, ξ, the dip, δ, and the rake, λ, of the faults are cited. Finally, the technique (Tech.) on which the determination of the fault strike is based (MA = macroseismic, CL = clusters, SF = surface faulting, FP = fault plane solutions), as well as the reference (Ref.) from which the information has been drawn are presented in the last two columns.

For those cases where the rupture strike was determined using more than one techniques, the adopted strike, ξ, for the fault plane was selected on the basis of the quality of the original data. The dip, δ, and the rake, λ, reported were those determined by the fault plane solution, if such information was available for the corresponding earthquake. When such a solution was not available, the dip and rake of the typical fault plane solution which holds for the area where the epicentre of the earthquake belongs was adopted (Papazachos et al., 1997c).

The ambiguity of distinguishing between fault plane and auxiliary plane, when fault plane solutions were available, has been solved by using the available additional seismological data (MA, CL, SF) or any other type of information (geologic, topographic). It must be noticed, however, that in several cases the dip direction of normal faults in the Aegean area or thrust faults along the north Ionian and the Adriatic coast (presented in Table 3), where both

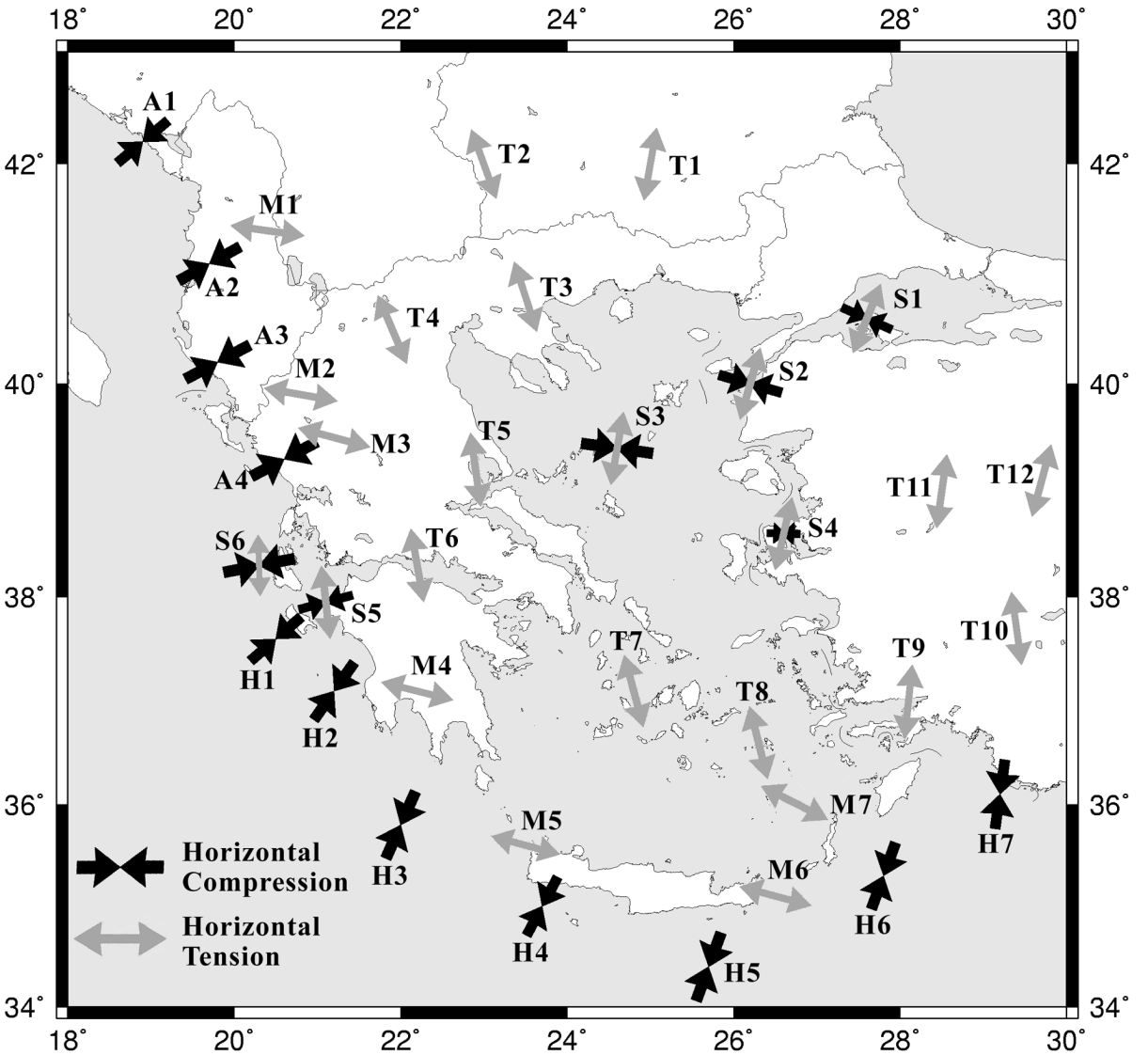

Fig. 4. The stress field in the Aegean and surrounding area. Horizontal compression dominates along the western coast of Albania and central Greece ($A_1, \ldots, A_4$) as well as along the convex side of the Hellenic arc ($H_1, \ldots, H_7$). North–south extension dominates in the Aegean area ($T_1, \ldots, T_{12}$) but along the Hellenides mountain range it changes and trends in an almost east–west direction ($M_1, \ldots, M_7$). Both maximum compression and maximum tension are almost horizontal along the Marmara–North Aegean area as well as in the Ionian islands where strike-slip faulting occurs ($S_1, \ldots, S_6$).

planes exhibit similar strike, may not be correct. Therefore, fault dipping in the opposite direction of that indicated in this table should always be considered as a possible alternative in these cases. For this reason rupture zones of the 150 shallow earthquakes of Table 3 and not the faults are presented in Fig. 5. In this figure, the fault rupture zones are separated into three main categories depending on the fault type (normal, strike-slip, thrust). Normal faults are represented by light grey ellipses, strike-slip faults by dark grey ellipses thrust faults are shown as solid black ellipses. Although macroseismic data were previously shown to be of similar accuracy when defining the direction of the rupture zone, we have separated the

Table 3
Parameters of the seismic faults for 150 shallow strong ($M \geq 6.0$) earthquakes in Greece and surrounding area

No.	Date	φ°_{N}, λ°_{E}	M	ζ	δ	λ	Tech.	Ref.
1	426 BC	38.85, 22.78	6.8	80	44	−88	MA	1
2	17 AD	38.63, 27.59	7.0	290	45	−97	MA	1
3	365, July 21	35.20, 23.20	8.3	315	29	124	CL	2
4	1303, Dec	36.10, 29.00	8.0	290	25	95	CL	2
5	1508, May 3	35.05, 25.70	7.5	307	35	99	MA	28
6	1509, Sep. 30	41.00, 28.80	7.4	112	64	−145	MA	1
7	1668, July 10	38.38, 27.17	6.8	260	46	−127	MA	28
8	1733, Dec. 23	37.10, 24.80	6.5	60	45	−92	CL	3
9	1735	36.80, 24.50	6.5	60	45	−92	CL	3
10	1752, Jul. 29	41.41, 26.61	7.5	62	37	−88	MA	1
11	1766, May 22	40.80, 29.10	7.3	102	64	−145	MA	28
12	1766, Aug.5	40.74, 27.11	7.6	59	64	−145	MA	1
13	1829, May 5	41.10, 24.50	7.3	83	37	−88	MA	1
14	1845, Oct. 11	39.10, 26.30	6.7	237	46	−127	MA	28
15	1858, Feb. 21	37.87, 22.88	6.5	236	42	−99	MA	1
16	1859, Aug. 21	40.10, 26.00	6.9	66	64	−145	MA	1
17	1861, Dec. 26	38.25, 22.16	6.7	288	30	−78	SF	4
18	1867, Feb. 4	38.39, 20.52	7.4	42	56	163	MA	28
19	1867, Mar. 7	39.25, 26.21	6.8	67	46	−127	MA	1
20	1870, Aug. 1	38.48, 22.55	6.8	83	30	−78	MA	1
21	1881, Apr. 3	38.30, 26.20	6.5	61	46	−127	MA	1
22	1886, Aug. 27	37.10, 21.50	7.5	324	29	124	MA	1
23	1889, Oct. 25	39.20, 25.90	6.8	246	46	−127	MA	28
24	1893, Feb. 7	40.59, 25.53	6.8	239	64	−167	MA	1
25	1893, Apr. 17	37.68, 20.81	6.5	10	42	−137	MA	28
26	1893, May 27	38.31, 23.25	6.3	61	42	−99	MA	1
27	1894, Apr. 20	38.60, 23.04	6.7	295	42	−70	SF	5
28	1894, Apr. 27	38.66, 23.04	7.2	295	42	−70	SF	5
29	1898, July 31	39.65, 20.80	6.3	320	43	98	MA	28
30	1899, Jan. 22	37.20, 21.60	6.5	335	29	124	MA	1
31	1899, Sep. 20	37.82, 28.25	7.0	90	36	−87	SF	6
32	1902, July 5	40.82, 23.04	6.5	71	37	−88	MA	28
33	1903, Nov. 25	42.14, 23.31	6.1	81	37	−88	MA	1
34	1904, Apr. 4	41.85, 23.00	7.1	93	37	−88	MA	1
35	1904, Apr. 4	41.80, 23.00	7.7	269	37	−88	MA	1
36	1904, Apr. 10	42.65, 22.83	6.0	86	37	−88	MA	1
37	1904, Aug. 11	37.66, 26.93	6.8	249	38	−96	MA	1
38	1905, Jan. 20	39.67, 22.83	6.2	336	44	−88	MA	1
39	1905, June 1	42.05, 19.50	6.6	324	18	94	MA	1
40	1905, Nov. 8	40.26, 24.33	7.5	72	64	−167	MA	28
41	1906, Sep. 28	40.90, 20.70	6.0	1	45	−104	MA	28
42	1906, Oct. 8	41.88, 23.06	6.4	86	44	−88	MA	28
43	1911, Feb.18	40.90, 20.80	6.7	3	40	−100	MA	1
44	1912, Jan. 24	38.11, 20.67	6.8	66	56	163	MA	1
45	1912, Aug. 9	40.62, 26.88	7.6	70	64	−145	SF	6
46	1914, Oct. 17	38.31, 23.34	6.0	82	42	−99	MA	1
47	1914, Nov.27	38.72, 20.62	6.3	16	60	165	MA	1
48	1915, Jan. 27	38.36, 20.60	6.6	35	56	163	MA	1
49	1915, Aug. 7	38.50, 20.62	6.7	49	56	163	MA	1
50	1917, Dec. 24	38.40, 21.70	6.0	68	85	−160	MA	1
51	1919, Feb. 24	37.40, 21.40	6.3	309	22	120	MA	1
52	1919, Nov. 18	39.20, 27.40	7.0	98	45	−97	MA	28

Table 3 (continued)

No.	Date	φ°_{N}, λ°_{E}	M	ζ	δ	λ	Tech.	Ref.
53	1921, Sep. 13	38.90, 21.18	6.0	165	44	−99	MA	1
54	1922, Dec. 7	41.71, 20.76	6.1	27	45	−104	MA	1
55	1923, Dec. 5	40.00, 23.40	6.4	40	64	−167	MA	1
56	1927, Feb.14	43.00, 18.00	6.1	294	18	94	MA	1
57	1927, July 1	36.78, 22.36	7.1	144	40	−81	MA	1
58	1928, Apr. 14	42.15, 25.28	6.8	90	37	−88	SF	5
59	1928, Apr. 18	42.10, 25.00	7.0	270	37	−88	SF	5
60	1928, Apr. 22	37.94, 22.98	6.3	247	42	−99	MA	1
61	1930, Feb. 23	39.60, 23.00	6.0	310	44	−88	MA	1
62	1930, Mar.31	39.47, 23.03	6.1	322	44	−88	MA	1
63	1930, Apr.17	37.78, 22.99	6.0	76	42	−99	MA	1
64	1931, Mar. 7	41.27, 22.31	6.0	65	37	−88	MA	1
65	1931, Mar. 8	41.28, 22.49	6.7	92	37	−88	MA	1
66	1932, Sep. 26	40.45, 23.76	7.0	90	−37	−88	SF	7
67	1932, Sep. 29	40.97, 23.27	6.2	80	37	−88	MA	1
68	1933,Apr. 23	36.80, 27.30	6.6	60	45	−92	MA	28
69	1933, May 11	40.62, 23.53	6.3	113	37	−88	MA	1
70	1938,July 20	38.29, 23.79	6.0	87	42	−99	MA	1
71	1941,Mar. 1	39.67, 22.54	6.3	143	44	−88	MA	1
72	1944,June 25	39.05, 29.26	6.1	290	42	−92	SF	8
73	1947, Oct. 6	36.96, 21.68	7.0	306	29	124	MA	1
74	1948, Apr. 22	38.71, 20.57	6.5	0	60	165	MA	28
75	1949, July 23	38.58, 26.23	6.7	250	46	−127	MA	28
76	1953, Mar.18	40.02, 27.53	7.4	250	70	−160	SF	5
77	1953, Aug. 9	38.30, 20.40	6.4	30	56	163	MA	1
78	1953, Aug.11	38.10, 20.60	6.8	159	22	120	MA	1
79	1953, Aug.12	38.30, 20.60	7.2	30	56	163	MA	1
80	1953, Oct. 21	38.30, 20.96	6.3	17	85	−160	MA	1
81	1954, Apr. 30	39.28, 22.29	7.0	246	44	−88	MA	1
82	1955, Apr. 19	39.37, 23.00	6.2	142	44	−88	MA	1
83	1955,July 16	37.55, 27.05	6.9	81	38	−96	MA	1
84	1956, July 9	36.64, 25.96	7.5	65	40	−90	FP	9
85	1957, Mar. 8	39.38, 22.63	6.8	277	44	−88	MA	1
86	1957, Apr. 24	36.40, 28.60	6.8	300	25	95	MA	1
87	1957, Apr. 25	36.50, 28.60	7.2	310	25	95	MA	1
88	1958, Aug. 27	37.40, 21.00	6.9	329	22	120	MA	1
89	1959, May 14	35.00, 24.72	6.3	309	35	99	MA	1
90	1959, Nov. 15	37.78, 20.53	6.8	46	37	−173	FP	10
91	1960, May 26	40.63, 20.65	6.5	3	44	−99	MA	1
92	1962, Mar. 18	40.67, 19.63	6.0	334	29	65	MA	28
93	1962, Apr. 10	37.80, 20.10	6.3	332	22	120	MA	1
94	1963, July 26	42.00, 21.40	6.1	29	44	−99	MA	1
95	1963, Sep. 18	40.67, 29.00	6.3	293	56	−99	FP	11
96	1964, Oct. 6	40.10, 27.93	6.9	273	46	−95	FP	12
97	1965, Mar. 9	39.16, 23.89	6.1	40	90	−174	FP	13
98	1965, Apr. 5	37.70, 22.00	6.1	226	57	−159	FP	13
99	1965, Apr. 9	35.13, 24.31	6.1	301	18	98	MA	1
100	1965, July 6	38.27, 22.30	6.3	281	34	−71	FP	14
101	1966, Feb. 5	39.10, 21.70	6.2	90	50	−85	FP	14
102	1966, Oct. 29	38.78, 21.11	6.0	324	40	48	FP	14
103	1967, Mar. 4	39.20, 24.60	6.6	98	54	−107	FP	13
104	1967, May 1	39.47, 21.25	6.4	2	36	−100	FP	12
105	1967, Nov. 30	41.39, 20.46	6.3	4	45	−105	FP	14

Table 3 (continued)

No.	Date	φ°_{N}, λ°_{E}	M	ζ	δ	λ	Tech.	Ref.
106	1968, Feb. 19	39.50, 25.00	7.1	217	86	175	FP	15
107	1968, Dec. 5	36.60, 26.90	6.0	86	50	−90	FP	13
108	1969, Jan. 14	36.10, 29.20	6.2	282	25	95	FP	13
109	1969, Mar. 3	40.10, 27.50	6.0	268	53	108	FP	11
110	1969, Mar. 23	39.13, 28.44	6.1	112	34	−90	FP	16
111	1969, Mar. 25	38.20, 28.40	6.0	90	40	−105	FP	13
112	1969, Mar. 28	38.29, 28.57	6.6	281	34	−90	SF	16
113	1969, June 12	34.40, 25.00	6.1	294	29	105	FP	13
114	1970, Mar. 28	39.16, 29.42	7.1	308	35	−90	SF	17
115	1970, Apr. 8	38.36, 22.53	6.2	278	20	−85	FP	17
116	1970, Apr.19	39.00, 29.80	6.0	104	34	−90	FP	16
117	1971, May 12	37.60, 29.70	6.2	68	40	−90	FP	12
118	1971, May 25	39.00, 29.70	6.1	96	37	−108	FP	16
119	1972, May 4	35.10, 23.60	6.5	308	18	90	FP	18
120	1972, Sep. 17	38.11, 20.31	6.3	46	66	−174	FP	10
121	1973, Nov. 29	35.18, 23.75	6.0	316	10	90	FP	17
122	1975, Mar. 27	40.40, 26.10	6.6	68	55	−145	FP	11
123	1976, May 11	37.40, 20.40	6.5	327	12	90	FP	10
124	1977, Sep. 11	34.90, 23.00	6.3	320	30	90	FP	12
125	1978, Jun. 20	40.61, 23.27	6.5	250	46	−70	SF	19
126	1979, Apr. 15	41.97, 19.00	7.1	317	15	90	FP	14
127	1979, May 24	42.20, 18.80	6.3	322	32	90	FP	14
128	1980, July 9	39.27, 22.83	6.5	81	40	−90	FP	20
129	1980, July 9	39.20, 22.60	6.1	81	40	−90	FP	20
130	1981, Feb. 24	38.07, 23.00	6.7	264	42	−80	SF	11
131	1981, Feb. 25	38.20, 23.10	6.4	241	44	−85	FP	11
132	1981, Mar. 4	38.18, 23.24	6.3	70	45	−90	SF	21
133	1981, Dec. 19	39.00, 25.26	7.2	37	67	−166	FP	22
134	1981, Dec. 27	38.90, 24.90	6.5	216	79	175	FP	11
135	1982, Jan. 18	39.78, 24.50	7.0	233	62	−173	FP	11
136	1983, Jan. 17	38.10, 20.20	7.0	40	45	168	FP	23
137	1983, Mar. 23	38.20, 20.30	6.2	29	68	174	FP	23
138	1983, July 5	40.30, 27.20	6.1	248	70	−155	FP	24
139	1983, Aug. 6	40.00, 24.70	6.8	228	89	−168	FP	25
140	1984, June 21	35.40, 23.30	6.2	322	16	114	FP	13
141	1986, Sep. 13	37.05, 22.11	6.0	200	50	−81	FP	26
142	1986, Oct. 11	37.90, 28.50	6.0	74	58	−140	FP	25
143	1988, Oct. 16	37.90, 20.90	6.0	32	87	−166	FP	25
144	1990, June 16	39.30, 20.60	6.0	329	39	102	FP	25
145	1990, Dec. 21	40.92, 22.36	6.0	45	52	−105	FP	25
146	1992, Apr. 30	35.10, 26.60	6.1	172	38	−106	FP	25
147	1992, Nov. 6	38.19, 27.05	6.2	238	85	−167	FP	25
148	1994, Sep. 1	41.18, 21.19	6.1	24	40	−90	MA	1
149	1995, May 13	40.16, 21.67	6.6	240	45	−101	FP	27
150	1995, June 15	38.37, 22.15	6.4	276	34	−73	FP	25

1. Papazachos et al. (1997c), 2. Papazachos (1996), 3. Papazachos and Panagiotopoulos (1993), 4. Schmidt (1867), 5. Richter (1958), 6. Ambraseys and Finkel (1987), 7. Maravelakis (1933), 8. Ambraseys (1988), 9. Shirokova (1972), 10. Papadimitriou (1993), 11. Taymaz et al. (1991), 12. Papazachos et al. (1991), 13. McKenzie (1972), 14. Baker et al. (1997), 15. Kiratzi et al. (1991), 16. Eyidogan and Jackson (1985), 17. McKenzie (1978), 18. Kiratzi and Langston (1989), 19. Kiratzi et al. (1985), 20. Papazachos et al. (1983), 21. Papazachos et al. (1984a), 22. Papazachos et al. (1984b), 23. Scordilis et al. (1985), 24. Dziewonski et al. (1984), 25. Harvard Solution, 26. Papazachos et al. (1988), 27. Geological Survey of Japan, 28. Papazachos and Papazachou (1997).

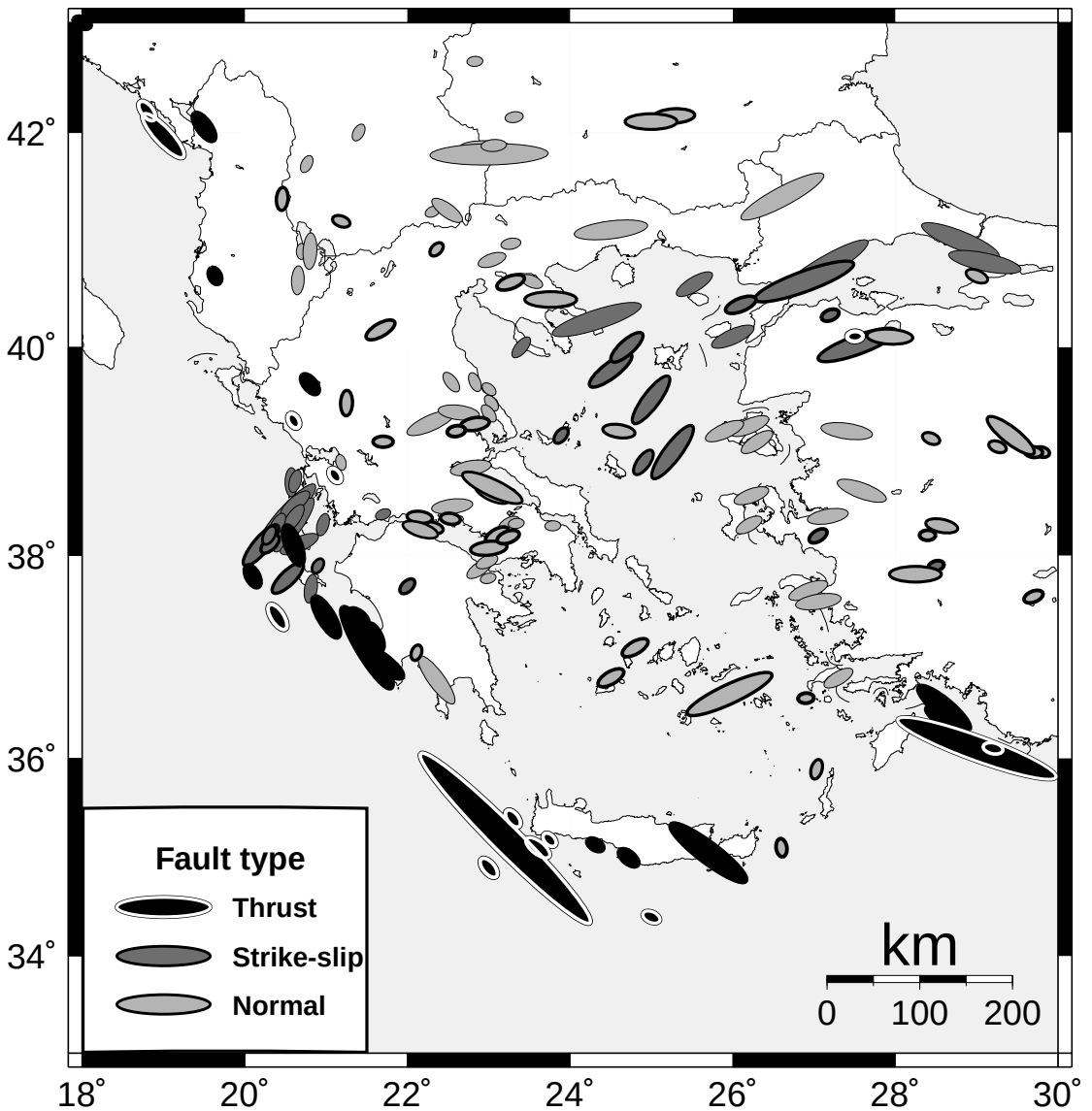

Fig. 5. Rupture (fault) zones in the Aegean area. The thrust zones along western Albania and the northwestern coast of central Greece have a northwest–southeast strike. These zones have the same strike along the western part of the Hellenic arc (Zante–Western Crete) and change to westnorthwest–eastsoutheast in its eastern part (East Crete–Rhodes). Tensional rupture zones which strike in an about east–west direction dominate in the Aegean but similar tensional zones with almost north–south strikes are observed along the Hellenides mountain chain, which changes to a northwest–southeast strike along the eastern coast of central Greece. Strike-slip rupture zones dominate in the Marmara–North Aegean troughs as well as in the Ionian islands (Cephalonia–Leukada–Zante).

rupture zones in Fig. 5 by drawing a thick border (black for normal and strike-slip faults, white for thrust faults) when a method other than the macroseismic was used (FP, CL, SF). For each ellipse the length and width are equal to the expected length and width of the corresponding fault. Since in the majority of cases these lengths or widths are not precisely known, they were determined from the moment magnitude, either estimated from waveform analysis or converted from local and surface magnitude by ap-

propriate formulas (Papazachos et al., 1997a), using Eqs. 1 and 2 which are applicable for the Balkan area. It should be noted that the width of the ellipses shown on the map is equal to the fault width and not to its horizontal projection on the surface, since the fault projection could not be distinguished for sub-vertical faults, mainly of strike-slip type.

6. Discussion and conclusions

In order to define the rupture zones of strong earthquakes in the Aegean area, the results of the application of four independent seismological techniques in 45 cases of strong shallow earthquakes ($M \geq 6.0$) were compared to check the validity of the techniques. This comparison indicated that the strike of the rupture zone of a strong shallow earthquake can be reliably calculated by application of any one of these four techniques if a good sample of data is available. It is important to notice that the use of macroseismic data shows an unexpected efficiency in determining the rupture direction, concerning the subjective character of macroseismic data. Moreover, the observed correlation of energy radiation (identified by macroseismic intensities) and fault direction suggests that this energy focusing is a systematic effect in the Aegean area, regardless of the type of faulting (normal, thrust or strike-slip). The only mechanism which can explain such a behaviour is the presence of significant along-fault rupture velocities (uni- or bi-directional) which have as a result the radiation of the relatively larger part of seismic energy (therefore macroseismic damage) along the fault rupture zone.

The four techniques have then been applied for the determination of the strike of the rupture zones of 150 strong ($M \geq 6.0$) shallow earthquakes in the Aegean area. Furthermore, published fault plane solutions were used to define the typical directions of the stress components (P and T axes) in several regions of the investigated area (Fig. 4). This as well as additional information (relations between dimensions of the fault and magnitude of the earthquake, etc.) were finally used to define the rupture zones of these 150 earthquakes (Fig. 5).

Figs. 4 and 5 represent our final results for the rupture zones of the Aegean area. Five seismotectonic regimes can be distinguished: the compressional regime along the east Adriatic and northern Ionian coastal area, the compressional regime along the Hellenic trench, the tensional regime in the broad Aegean area, the tensional regime along the Hellenides mountain range and the regime of strike-slip dextral faulting along the belt which crosses northern Aegean in a northeast–southwest direction.

In the coastal area along the eastern boundary of the Adriatic sea and northern Aegean sea (west Albania–west mainland of Greece) maximum compression (Fig. 4) is horizontal and normal to the trend of the coast ($\bar{\zeta} = 238^{\circ}$, $\bar{\vartheta} = 14^{\circ}$). This is a continent–continent collision which is due to the convergence between the Apulian plate which is rotated in an anticlockwise way (Ritsema, 1974; McKenzie, 1972, 1978; Taymaz et al., 1990, 1991) and/or to the western motion of Anatolia which is transferred across northern Greece and Albania and results in a collision against the Apulian platform (Smith et al., 1994; Le Pichon et al., 1995). Rupture zones in this belt are of thrust type and oriented parallel to the coast (Fig. 5). These thrust faults may dip to the southwest or the northeast.

The compressional field along the Hellenic trench is horizontal and trends in a northeast–southwest direction ($\bar{\zeta} = 206^{\circ}$, $\bar{\vartheta} = 18^{\circ}$). This field is partly due to subduction of the front part of the African lithosphere (front oceanic part of the eastern Mediterranean lithosphere) under the Aegean lithosphere but mainly to the overriding of the Aegean plate on the African plate (McKenzie, 1970; Smith et al., 1994; Papazachos, 1999). Rupture thrust zones in this belt have a northwest strike in the western part of the trench and a west-northwest strike in the eastern part of the arc (see Fig. 5).

Along the Hellenides mountains tension is horizontal and trends in an almost east–west direction ($\bar{\zeta} = 105^{\circ}$, $\bar{\vartheta} = 6^{\circ}$) and rupture zones (normal faults) strike in an about north–south direction. The belt consists of two parts, the northern (eastern Albania–northwestern Greece) and the southern (Cretan trough) because it is interrupted in central Greece. Several proposals were made to interpret this east–west expansion in the southern part (southern Aegean) of this belt (Lyon-Caen et al., 1988; Armijo et al., 1992; Kastens et al., 1999; Hatzfeld et al., 1997). All these proposals are based on the

assumption of an ocean–continent collision which does not hold for the northern part of this belt where this regime retains the same properties (see Figs. 1 and 4). Therefore, the genetic causes of this east–west expanding belt are still an open question.

The back-arc Aegean and surrounding area is dominated by north–south extension ($\bar{\zeta} = 354^o$, $\bar{\tau} = 4^o$) and most seismic faults have an east–west strike there. Recent GPS and seismological observations has shown that the Aegean lithosphere is moving fast to a southwest direction relative to Europe (Jackson, 1994; Smith et al., 1994; Reilinger et al., 1997; Papazachos, 1999). The south-westward motion and the expansion of the Aegean lithosphere is probably due to gravitation spreading or gravitational collapse of the expanding area due to roll back of the descending lithospheric plate towards the remaining scarp of the oceanic crust beneath the Ionian sea (Le Pichon and Angelier, 1981; Dewey, 1988). This idea is supported by recent tomographic results for this area (Papazachos and Nolet, 1997).

Not all rupture zones in the Aegean (normal faults) strike in an east–west direction (Fig. 5). This is probably due to the fact that some of the active faults existed before the occurrence of the presently active tectonic stress field and their orientation was determined by the stress field of that time. As a typical example of this effect of the pre-existing tectonic fabric we refer to the Atalanti (central Greece) fault where the April 27, 1984 ($M = 7.2$) earthquake occurred. This fault is 55 km long, it strikes WNW ($\zeta = 295^o$) and dips NNE. Under the effect of the presently acting N–S extension, a normal faulting with a strike-slip sinistral component is expected. Detailed field observations made immediately after the generation of this earthquake showed that the rupture was really of that type (Richter, 1958).

Along the strike-slip belt, faults are almost vertical and of dextral type ($\bar{\zeta} = 47^o$, $\bar{\delta} = 88^o$, $\bar{\lambda} = 176^o$), in agreement with a fast southwest motion of the Aegean plate relatively to Eurasia. In central Greece, however, north–south extension (normal faulting) dominates and for this reason this strike-slip belt is composed of two separate branches, the northeast (northwest Anatolia–north Aegean) branch and the southwest branch which is dominated by the Cephalonia Transform Fault (CTF) (Scordilis et al., 1985).

Acknowledgements

The authors would like to express their gratitude to D. Pantosti, W. Bakun and T. Taymaz, for their fruitful comments on the manuscript, which contributed to the improvement of the paper. All the maps were created using GMT (Generic Mapping Wessel and Smith, 1995), geophysical freeware mapping software, and we are indebted to its authors, P. Wessel and W. Smith, for making this software available to the geophysical community. This work has been partially funded by the EU Environment Research Project ENV4-CT96-0277.

References

Ambraseys, N.N., 1988. Engineering seismology. Earthquake Eng. Struct. Dyn. 17, 1–105.

Ambraseys, N.N., Finkel, C.F., 1987. Seismicity of Turkey and neighbouring regions, 1899–1915. Ann. Geophys. 5, 701–726.

Armijo, R., Lyon-Caen, H., Papanastasiou, D., 1992. East–west extension and Holocene normal-fault scarps in the Hellenic arc. Geology 20, 491–494.

Baker, C., Hatzfeld, D., Lyon-Caen, H., Papadimitriou, E., Rigo, A., 1997. Earthquake mechanisms of the Adriatic sea and western Greece. Geophys. J. Int. 131, 559–595.

Benioff, H., 1955. Mechanism and strain characteristics of the White Wolf fault as indicated by the aftershock sequence. In: Earthquakes in Kern County, California, During 1952. Calif. Dep. Natl. Res. Div. Mines Bull., 171, 199–202.

Benioff, H., 1962. Movements on major transcurrent faults. Continental Drift. Int. Geophys. Ser., Academic Press, New York, 3, 103–134.

Caputo, R., Pavlides, S., 1991. Neotectonics and structural evolution of Thessaly (Central Greece). Bull. Geol. Soc. Greece 25, 119–133.

Clark, P.J., Paradissis, D., Briole, P., England, P.C., Parsons, B.E., Billiris, H., Veis, G., Ruegg, J.C., 1997. Geodetic investigation of the 13 May 1995 Kozani–Grevena (Greece) earthquake. Geophys. Res. Lett. 24, 07–710.

Dewey, J.F., 1988. Extensional collapse of orogens. Tectonics 7, 1123–1139.

Dziewonski, A., Franzen, J., Woodhouse, J., 1984. Centroid-moment tensor solutions for July–September, 1983. Phys. Earth Planet. Inter. 34, 1–8.

Eyidogan, H., Jackson, J., 1985. A seismological study of normal faulting in the Demirci, Alasehir and Gediz earthquakes of 1960–1970 in western Turkey; implications for the nature and geometry of deformation in the continental crust. Geophys. J. R. Astron. Soc. 81, 569–607.

Gzovsky, M.V., 1962. Tectonophysics and earthquake forecasting. Bull. Seismol. Soc. Am. 52, 485–505.

Hatzfeld, D., Karakostas, V., Ziazia, M., Selvaggi, G., Leborgne,

S., Berge, C., Guiguet, R., Paul, A., Voidomatis, P., Diagourtas, D., Kassaras, I., Koutsikos, I., Makropoulos, K., Azzara, R., Bona, M.D., Baccheschi, S., Bernard, P., Papaioannou, C., 1996. The Kozani–Grevena (Greece) earthquake of 13 May 1995 revisited from a detailed seismological study. Bull. Seismol. Soc. Am. 87, 463–473.

Hatzfeld, D., Martinod, J., Bastet, G., 1997. An analog experiment for the Aegean to describe the contribution of gravitational potential energy. J. Geophys. Res. 102, 649–659.

Jackson, J., 1994. Active tectonics of the Aegean region. Annu. Rev. Earth Planet. Sci. 22, 239–271.

Karakaisis, G.F., Karakostas, B.G., Papadimitriou, E.E., Papazachos, B.C., 1985. Properties of the 1979 Monte Negro seismic sequence. Pure Appl. Geophys. 122, 25–35.

Kastens, K.A., Gilbert, L.E., Hurst, K.J., Veis, G., Paradissis, D., Billiris, H., Schluter, W., Seeger, H., 1999. GPS evidence for arc-parallel extension along the Hellenic arc, Greece, Tectonophysics (submitted).

Kelleher, J.A., 1972. Rupture zones of large south american earthquakes and some predictions. J. Geophys. Res. 77, 2087–2103.

Kiratzi, A.A., Langston, C.A., 1989. Estimation of earthquake source parameters of the May 4, 1972 event of the Hellenic arc by the inversion of waveform data. Phys. Earth Planet. Inter. 57, 225–232.

Kiratzi, A.A., Karakaisis, G.F., Papadimitriou, E.E., Papazachos, B.C., 1985. Seismic source-parameter relations for earthquakes in Greece. Pure Appl. Geophys. 123, 27–41.

Kiratzi, A.A., Wagner, G., Langston, C.A., 1991. Source parameters of some large earthquakes in Northern Aegean determined by body waveform inversion. Pure Appl. Geophys. 135, 515–527.

Kudo, K., 1983. Seismic source characteristics of recent major earthquakes in Turkey. In: Ohta, Y. (Ed.), A Comprehensive Study on Earthquake Disasters in Turkey in View of Seismic Risk Reduction. Dep. Archit. Eng., Fac. Eng., Hokkaido Univ., Sapporo, Japan, pp. 23–66.

Le Pichon, X., Angelier, J., 1981. The Aegean Sea. Philos. Trans. R. Soc. London 30, 357–372.

Le Pichon, X., Chamot-Rooke, N., Lallemant, S., Noomen, R., Veis, G., 1995. Geodetic determination of the kinematics of central Greece with respect to Europe: Implications for eastern Mediterranean tectonics. J. Geophys. Res. 100, 12675–12690.

Lyon-Caen, H., Armijo, R., Drakopoulos, J., Baskoutas, J., Delibasis, N., Ganlon, R., Kouskouna, V., Latoussakis, J., Makropoulos, K., Papadimitriou, P., Papanastasiou, D., Pedotti, G., 1988. The 1986 Kalamata (South Peloponnesus) earthquake: Detailed study of a normal fault, evidence for east–west extension in the Hellenic Arc. J. Geophys. Res. 93, 14967–15000.

Maravelakis, J.M., 1933. The Geologic and Macroseismic Characters of the Earthquakes of Chalkidiki, September 1932. O. Theodorou, Thessaloniki, 1, 33 pp. (in Greek).

McKenzie, D.P., 1970. The plate tectonics of the Mediterranean region. Nature 226, 239–243.

McKenzie, D.P., 1972. Active tectonics of the Mediterranean region. Geophys. J. R. Astron. Soc. 30, 109–185.

McKenzie, D.P., 1978. Active tectonics of the Alpine–Himalayan belt: the Aegean Sea and surrounding regions. Geophys. J. R. Astron. Soc. 55, 217–254.

Mountrakis, D., Psilovikos, A., Papazachos, B.C., 1983. The geotectonic regime of the 1978 Thessaloniki earthquake. In: Papazachos, B.C., Carydis, P.G. (Eds.), The Thessaloniki, Northern Greece, Earthquake of June 20, 1978 and its Seismic Sequence. Tech. Chamber Greece, Thessaloniki, Greece, pp. 11–27.

Papadimitriou, E.E., 1993. Focal mechanism along the convex side of the Hellenic arc and its tectonic significance. Bull. Geof. Teor. Appl. 35, 401–426.

Papazachos, B.C., 1989. Measures of earthquake size in Greece and surrounding areas. Proc. 1st Sci. Conf. Geophysics. Geophys. Soc. Greece, April 19–21, Athens, Greece, 1, 438–447.

Papazachos, B.C., 1996. Large seismic faults in the Hellenic arc. Ann. Geofis. 39, 891–903.

Papazachos, B.C., Panagiotopoulos, D.G., 1993. Normal faults associated with volcanic activity and deep rupture zones in the southern Aegean volcanic arc. Tectonophysics 220, 301–308.

Papazachos, B.C., Papazachou, C.B., 1997. The Earthquakes of Greece. Ziti Publ., Thessaloniki, Greece, 304 pp.

Papazachos, B.C., Panagiotopoulos, D.G., Tsapanos, T.M., Mountrakis, D.M., Dimopoulos, G.C., 1983. A study of the 1980 summer seismic sequence in the Magnesia region of central Greece. Geophys. J. R. Astron. Soc. 75, 155–168.

Papazachos, B.C., Comninakis, P.E., Papadimitriou, E.E., Scordilis, E.M., 1984a. Properties of the February–March 1981 seismic sequence in the Alkyonides gulf of central Greece. Ann. Geophys. 2, 537–544.

Papazachos, B.C., Kiratzi, A.A., Voidomatis, P.S., Papaioannou, C.A., 1984b. A study of the December 1981–January 1982 seismic activity in northern Aegean Sea. Boll. Geof. Teor. Appl. 26, 101–113.

Papazachos, B.C., Kiratzi, A., Karakostas, B., Panagiotopoulos, D., Scordilis, E., Mountrakis, D., 1988. Surface fault traces, fault plane solution and spatial distribution of the aftershocks of the September 13, 1986 earthquake of Kalamata. Pure Appl. Geophys. 126, 55–68.

Papazachos, B.C., Kiratzi, A., Papadimitriou, E., 1991. Regional focal mechanisms for earthquakes in the Aegean area. Pure Appl. Geophys. 136, 405–420.

Papazachos, B.C., Hatzidimitriou, P.M., Karakaisis, G.F., Papazachos, C.B., Tsokas, G.N., 1993. Rupture zones and active crustal deformation in southern Thessalia, central Greece. Bull. Geof. Teor. Appl. 139, 363–374.

Papazachos, B.C., Kiratzi, A.A., Karakostas, B.G., 1997a. Toward homogeneous moment-magnitude determination for earthquakes in Greece and surrounding area. Bull. Seismol. Soc. Am. 87, 474–483.

Papazachos, B.C., Papaioannnou, C.A., Papazachos, C.B., Savvaidis, A.S., 1997b. Atlas of isoseismal maps for strong ($M \geq 5.5$) shallow ($h < 60$ km) earthquakes in Greece and surrounding area, 426 BC–1995. Publ. Geophys. Lab., Univ. Thessaloniki, 4, 176 pp.

Papazachos, B.C., Papadimitriou, E.E., Kiratzi, A., Papazachos, C.B., 1997c. The stress field in the Aegean area as deduced

from fault plane solutions of shallow earthquakes. IASPEI 29th General Assembly, Thessaloniki, 18–28 August 1997.

Papazachos, B.C., Karakostas, B.G., Kiratzi, A.A., Papadimitriou, E.E., Papazachos, C.B., 1998. A model for the 1995 Kozani–Grevena seismic sequence. J. Geodyn. 26, 217–231.

Papazachos, C.B., 1992. Anisotropic radiation modelling of macroseismic intensities for estimation of the attenuation structure of the upper crust in Greece. Pure Appl. Geophys. 138, 445–469.

Papazachos, C.B., 1999. The active crustal deformation field of the Aegean area inferred from seismicity and GPS data. J. Geophys. Res. (submitted).

Papazachos, C.B., Nolet, G.P., 1997. P and S deep velocity structure of the Hellenic area obtained by robust nonlinear inversion of travel times. J. Geophys. Res. 102, 8349–8367.

Pavlides, S., Zouros, N., Chatzipetros, A., Kostopoulos, D.S., 1995. The 13 May 1995 western Macedonia, Greece (Kozani–Grevena) earthquake; preliminary results. Terra Nova 7, 544–549.

Reilinger, R.E., McClusky, S.C., Oral, M.B., King, R.W., Toksoz, M.N., Barka, A.A., Kinik, I., Lenk, O., Sanli, I., 1997. Global Positioning System measurements of present-day crustal movements in the Arabia–Africa–Eurasia plate collision zone. J. Geophys. Res. 102, 2983–2999.

Richter, C.F., 1958. Elementary Seismology. Freeman, San Francisco, 768 pp.

Ritsema, A.R., 1974. The earthquake mechanism of the Balkan region. R. Neth. Meteorol. Inst. Sci. Rep. 74, 1–36.

Rocca, A.C., Karakaisis, G.F., Karakostas, B.G., Kiratzi, A.A., Scordilis, E.M., Papazachos, B.C., 1985. Further evidence on the strike-slip faulting of the northern Aegean through based on properties of the August–November 1983 seismic sequence. Boll. Geof. Teor. Appl. 27, 101–109.

Schmidt, J., 1867. Treatise on the 26(14) December 1861 earthquake of Aeghio. National Printing House, Athens, 51 pp. (in Greek and German).

Scordilis, E.M., Karakaisis, G.F., Karakostas, B.G., Panagiotopoulos, D.G., Comninakis, P.E., Papazachos, B.C., 1985. Evidence for transform faulting in the Ionian Sea. The Cephalonia island earthquake sequence of 1983. Pure Appl. Geophys. 123, 388–397.

Shirokova, E., 1972. Stress pattern and probable motion in the earthquake foci of the Asia–Mediterranean seismic belt. In: Balakina, L.M. et al. (Eds.), Elastic Strain Field of the Earth and Mechanisms of Earthquake Sources. Nauka, Moscow, Vol. 8.

Smith, D.E., Kolenkiewicz, R., Robbins, J.W., Dumm, P.J., Torrence, M.H., 1994. Horizontal crustal motion in the central and eastern Mediterranean inferred from satellite laser ranging measurements. Geophys. Res. Lett. 21, 1979–1982.

Soufleris, C., Stewart, G., 1981. A source study of the Thessaloniki (N. Greece) 1978 earthquake sequence. Geophys. J. R. Astron. Soc. 67, 343–358.

Taymaz, T., Jackson, J., Westaway, R., 1990. Earthquake mechanisms in the Hellenic trench near Crete. Geophys. J. Int. 102, 695–731.

Taymaz, T., Jackson, J., McKenzie, D., 1991. Active tectonics of the north and central Aegean Sea. Geophys. J. Int. 106, 433–490.

Wessel, P., Smith, W., 1995. New Version of the Generic Mapping Tools Released. Eos Trans. Am. Geophys. Union, 76, 329 pp.